Report

Current Biology

Early Evolution of Modern Birds Structured by Global Forest Collapse at the End-Cretaceous Mass Extinction

Highlights

- The end-Cretaceous mass extinction devastated forest habitats globally
- Tree-dwelling birds failed to persist across the end-Cretaceous extinction event
- All bird groups that survived the end-Cretaceous extinction were non-arboreal
- The early ancestors of many modern tree-dwelling bird groups were ground-dwelling

Authors

Daniel J. Field, Antoine Bercovici, Jacob S. Berv, ..., Tyler R. Lyson, Vivi Vajda, Jacques A. Gauthier

Correspondence

d.j.field@bath.ac.uk

In Brief

Field et al. show that the end-Cretaceous (K-Pg) mass extinction profoundly influenced the evolutionary history of modern birds. The K-Pg devastated global forests, and as a result no lineages of tree-dwelling birds survived the mass-extinction event. All modern tree-dwelling birds are descended from surviving ground-dwelling lineages.

Field et al., 2018, Current Biology *28*, 1–7
June 4, 2018
https://doi.org/10.1016/j.cub.2018.04.062

CellPress

Please cite this article in press as: Field et al., Early Evolution of Modern Birds Structured by Global Forest Collapse at the End-Cretaceous Mass Extinction, Current Biology (2018), https://doi.org/10.1016/j.cub.2018.04.062

Current Biology
Report

Early Evolution of Modern Birds Structured by Global Forest Collapse at the End-Cretaceous Mass Extinction

Daniel J. Field,[1,9,*] Antoine Bercovici,[2] Jacob S. Berv,[3] Regan Dunn,[4] David E. Fastovsky,[5] Tyler R. Lyson,[6] Vivi Vajda,[7] and Jacques A. Gauthier[8]

[1]Milner Centre for Evolution, Department of Biology and Biochemistry, University of Bath, Bath BA2 7AY, UK
[2]Department of Paleobiology MRC-121, National Museum of Natural History, Smithsonian Institution, 10th Street and Constitution Avenue NW, Washington, DC 20560-0121, USA
[3]Department of Ecology & Evolutionary Biology, Cornell University, 215 Tower Road, Ithaca, NY 14853, USA
[4]Integrated Research Center, Field Museum of Natural History, 1400 South Lake Shore Drive, Chicago, IL 60605, USA
[5]Department of Geosciences, University of Rhode Island, 9 East Alumni Avenue, Kingston, RI 02881, USA
[6]Department of Earth Sciences, Denver Museum of Nature and Science, 2001 Colorado Boulevard, Denver, CO 80205, USA
[7]Department of Palaeobiology, Swedish Museum of Natural History, Svante Arrhenius Väg 9, 104 05 Stockholm, Sweden
[8]Department of Geology & Geophysics, Yale University 210 Whitney Avenue, New Haven, CT 06511, USA
[9]Lead Contact
*Correspondence: d.j.field@bath.ac.uk
https://doi.org/10.1016/j.cub.2018.04.062

SUMMARY

The fossil record and recent molecular phylogenies support an extraordinary early-Cenozoic radiation of crown birds (Neornithes) after the Cretaceous-Paleogene (K-Pg) mass extinction [1–3]. However, questions remain regarding the mechanisms underlying the survival of the deepest lineages within crown birds across the K-Pg boundary, particularly since this global catastrophe eliminated even the closest stem-group relatives of Neornithes [4]. Here, ancestral state reconstructions of neornithine ecology reveal a strong bias toward taxa exhibiting predominantly non-arboreal lifestyles across the K-Pg, with multiple convergent transitions toward predominantly arboreal ecologies later in the Paleocene and Eocene. By contrast, ecomorphological inferences indicate predominantly arboreal lifestyles among enantiornithines, the most diverse and widespread Mesozoic avialans [5–7]. Global paleobotanical and palynological data show that the K-Pg Chicxulub impact triggered widespread destruction of forests [8, 9]. We suggest that ecological filtering due to the temporary loss of significant plant cover across the K-Pg boundary selected against any flying dinosaurs (Avialae [10]) committed to arboreal ecologies, resulting in a predominantly non-arboreal post-extinction neornithine avifauna composed of total-clade Palaeognathae, Galloanserae, and terrestrial total-clade Neoaves that rapidly diversified into the broad range of avian ecologies familiar today. The explanation proposed here provides a unifying hypothesis for the K-Pg-associated mass extinction of arboreal stem birds, as well as for the post-K-Pg radiation of arboreal crown birds. It also provides a baseline hypothesis to be further refined pending the discovery of additional neornithine fossils from the Latest Cretaceous and earliest Paleogene.

RESULTS

Neornithine Ecological Selectivity across the K-Pg

Ancestral ecological reconstructions (AERs) using recent time-scaled avian phylogenies [2, 11] under likelihood, maximum-parsimony, and Bayesian stochastic mapping frameworks yielded a clear ecological signal across the Cretaceous-Paleogene (K-Pg) boundary (Figure 1 and Supplemental Information). The deepest nodes within Neornithes are inferred to be predominantly non-arboreal, in terms of both general lifestyle and nesting substrate, including the most recent common ancestor (MRCA) of Neornithes (the crown bird root node), and the MRCAs of Palaeognathae (ostriches and kin), Neognathae (all non-palaeognath Neornithes), and Neoaves (all neognaths, excluding ducks, chickens, and their close relatives). Numerous independent transitions toward predominant arboreality are inferred for deep nodes within Neoaves early in the Cenozoic, including the extremely speciose and largely arboreal Inopinaves (a major clade of "core land birds" inferred to have transitioned to predominant arboreality by 64 million years ago) [2]. These results are robust to ongoing phylogenetic uncertainty with regard to neoavian interrelationships and divergence times [1, 2, 11, 12].

Terrestrial Antecedents for Numerous Modern Arboreal Bird Clades

Our AERs identify several extant clades with inferred transitions to arboreality early in the Cenozoic. Some of these clades, such as Otidimorphae (turacos, cuckoos, and bustards) and Telluraves (all Inopinaves except the Hoatzin), are represented by early-diverging crown clade fossils from the early Paleogene. The earliest well-constrained crown neoavian fossil (the stem

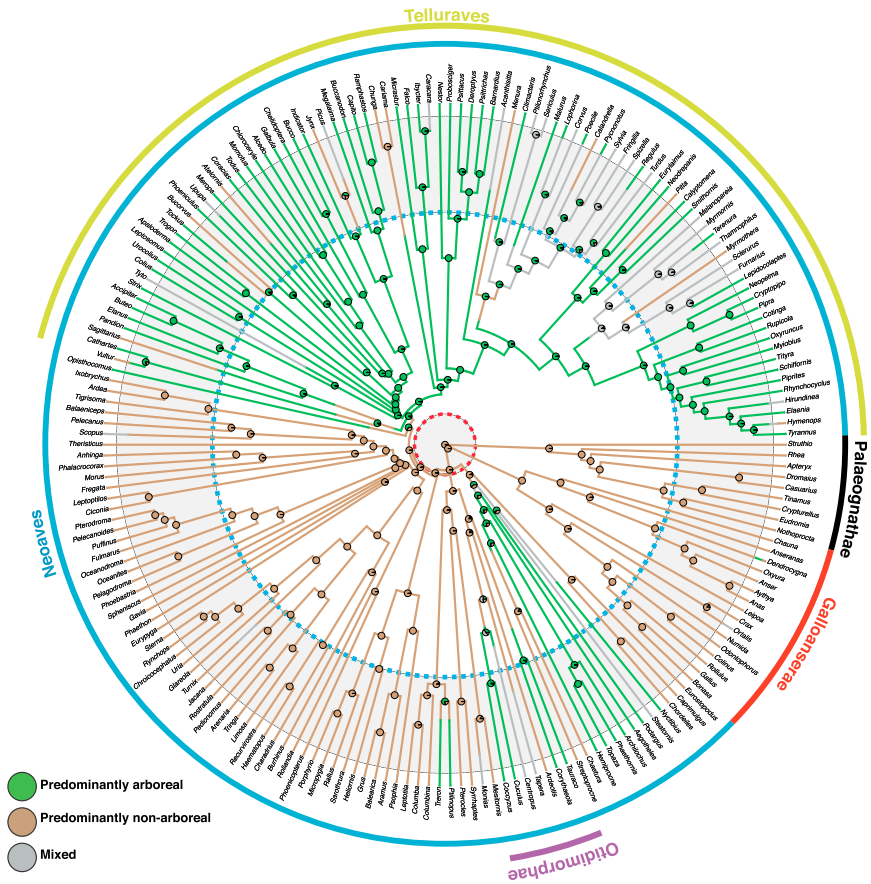

Figure 1. Ancestral Ecological Reconstructions Reveal Bias toward Non-arboreal Birds across the K-Pg

Bayesian ancestral ecological reconstructions (AERs) indicate that the most deeply diverging crown bird clades, including Neornithes (all crown birds), Neognathae (Galloanserae + Neoaves), and Neoaves, were ancestrally non-arboreal (pp > 0.99 for each node), with numerous independent transitions toward arboreality arising in the early Cenozoic, presumably after global forests had recovered from the Chicxulub impact. Concentric background rings demarcate geologic periods: the inner gray circle at the center indicates the Late Cretaceous, with the K-Pg boundary (66.02 Ma) indicated by the red dashed line; the white ring indicates the Paleogene (66.02–23.03 Ma), separated from the Neogene (23.03–2.58 Ma) by the dashed blue line. Tips extend to the present. Pie charts at the nodes indicate SIMMAP posterior probabilities for ancestral ecology, under our model. Branch colors represent a single randomly sampled stochastic character map from a posterior sample of 1,000 maps. The underlying phylogeny and taxonomy follow [2]; qualitatively identical patterns are inferred using an alternative phylogenetic hypothesis [11]. See also Figures S2–S4, as well as http://doi.org/10.5281/zenodo.1204464 for alternative reconstructions.

mousebird *Tsidiiyazhi abini*) is inferred by Ksepka and colleagues to be predominantly arboreal [3]. However, that study also suggests that the advanced zygodactyl and semizygodactyl perching specializations of *T. abini* and other arboreal members of Telluraves are the product of multiple independent origins in the Paleocene and Eocene. Additionally, hindlimb proportions among Otidimorphae covary with degrees of arboreality and terrestriality (D.J.F., unpublished data; Figure 2) and indicate that the earliest known crown otidimorph, the stem turaco *Foro panarium*, was most likely ground dwelling, despite arboreality predominating among extant turacos.

Assessing the Extent and Timeline of K-Pg Forest Collapse

Palynological data from K-Pg boundary sections worldwide reveal a vegetation response with a fern spike and floral turnover [14], which together indicate forest destruction on a global scale and a protracted (~1,000 year) onset of the recovery of climax vegetation [15]. We assessed the response of forest communities to the Chicxulub impact in the western interior of North America by conducting high-resolution relative abundance palynological analyses (down to 1 cm sampling intervals immediately above and below the boundary) of the John's Nose K-Pg boundary section in southwestern North Dakota (Figure 3). The North American K-Pg boundary sections constitute the best high-resolution record of the K-Pg transition in terrestrial ecosystems [17], and John's Nose is one of two sections in southwestern North Dakota that preserve the boundary clay and impact spherules, providing direct evidence of the Chicxulub impact. The palynological record shows the K-Pg boundary fern spike (*Cyathidites* sp. and *Laevigatosporites* sp., >70%) 2–7 cm above the boundary and floral turnover from 7 cm above the boundary, as indicated by the disappearance of typical Cretaceous pollen (K-taxa) and the dominance of new pollen types in the earliest Paleocene (*Ulmipollenites krempii*, *Kurtzipites circularis*, *K. trispissatus*, *Taxodiaceaepollenites* sp., and bisaccate pollen grains; Table S1).

DISCUSSION

Synthesis of recent results from paleontological studies and molecular divergence time analyses supports a major influence of the end-Cretaceous asteroid impact on near-crown and early crown bird evolution [1, 2, 4, 18, 19]. Fossil evidence suggests that the entirety of the neornithine stem group—including pterosaurs and all non-neornithine dinosaurs—perished in the aftermath of the impact [20], 66.02 Ma [15]. This includes even the crownward-most Mesozoic avialans outside of living bird diversity, such as Ichthyornithes (*Ichthyornis* and kin), Hesperornithes (*Hesperornis* and kin), Palintropiformes (relatives of *Palintropus retusus* and *Apsaravis ukhaana*), and the diverse and globally widespread Enantiornithes ("opposite birds"), which persisted into the terminal Cretaceous (Maastrichtian) [4] (Figure 4). Although the very deepest phylogenetic divergences within

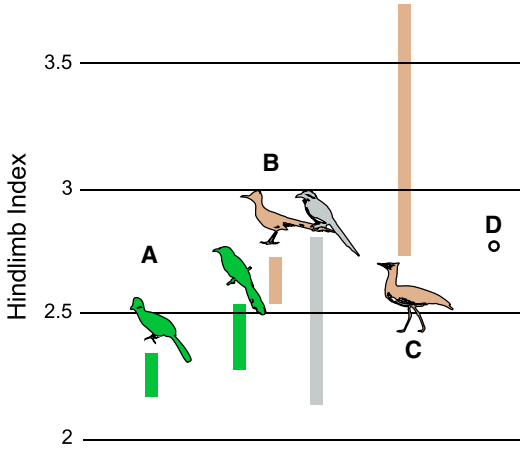

Figure 2. Hindlimb Ecomorphology Suggests Delayed Transitions toward Arboreality among Cenozoic Crown Birds

Early Cenozoic fossils of some modern lineages exhibiting largely arboreal habits suggest that their early antecedents were most likely ground dwelling [3, 13]. Hindlimb indices ((tarsometatarsus length + tibiotarsus length) / femur length) are plotted for the major clades within crown Otidimorphae—turacos (A; strictly arboreal), cuckoos (B; exhibiting arboreal, non-arboreal, and mixed members), and bustards (C; strictly ground dwelling)—as well as the early-Eocene stem turaco *Foro panarium* (D). *F. panarium* exhibits elongated hindlimb proportions greatly exceeding the range of extant turacos and arboreal cuckoos, suggesting non-arboreal habits. Predominantly arboreal taxa are green, predominantly non-arboreal are brown, and "mixed" are gray. See also Table S2.

Neornithes most likely took place during the Mesozoic, such as the divergence between Palaeognathae and Neognathae (the neornithine root node) and that between Galloanserae and Neoaves (the deepest divergence within Neognathae), virtually the entirety of the avian crown-group fossil record is restricted to sediments of Cenozoic age, and the earliest well-supported crown bird fossil is scarcely older than the end-Cretaceous, at approximately 67 Ma [3, 23].

Factors Influencing the Post-Cretaceous Survival of Crown Birds

Despite accumulating evidence for the dramatic influence of the Chicxulub asteroid impact on the evolutionary history of the neornithine total clade, little is known about either the factors that drove crownward stem birds such as enantiornithines to extinction or the biological attributes of early crown birds that survived the mass extinction and radiated in its wake. Recently, selection for the toothless bill that characterizes crown birds was posited as a potential factor favoring crown bird survivorship over other contemporaneous small theropods [24]. This argument suggests that the bill would have facilitated feeding on the hardy seeds and grains that may have been available as a food source in the immediate aftermath of the asteroid impact. Although this may be true, such a scenario ignores the fact that teeth do not preclude granivory (some toothed avialans are known to have fed on seeds [25]) and that a toothless bill was acquired multiple times among Mesozoic Avialae, including among derived enantiornithines [26]. Additionally, work incorporating fossil body-size estimates, ancestral state reconstructions, and rates of molecular evolution suggests that birds surviving the K-Pg mass extinction underwent transient selection and filtering for reduced body size (a Lilliput effect) [19], which may have facilitated avian survival by transiently reducing their total energetic requirements. Research on the evolution of neornithine breeding habits [27] suggests that relative to Enantiornithes, ancestral crown birds may have acquired proportionally larger eggs and alternative nesting substrates. Moreover, evolution of a crown-grade alimentary system has additionally been posited as a factor that may have influenced the post-K-Pg survival of Neornithes [28]; both of these latter hypotheses are tantalizing and warrant additional research.

Although all of the scenarios described above are plausible and not mutually exclusive, none fully explain the differential survivorship of early crown birds relative to crownward stem birds such as enantiornithines (which, despite differences in biological attributes such as skeletal pneumaticity and growth rates, were most likely biologically similar to Neornithes and probably more diverse and widespread in the terminal Cretaceous) [4]. Alone, these scenarios reveal an incomplete picture of broad-scale ecological selectivity among the crown birds that survived the K-Pg mass extinction.

We propose a new hypothesis regarding the extinction of stem birds and the survival of crown birds across the K-Pg boundary: namely, that global deforestation caused by the Chicxulub impact induced a selective filter against the survival of arboreal birds. Given compelling evidence for transient asteroid-impact-induced deforestation coincident with the end-Cretaceous mass extinction (Figure 3), the selective consequences of widespread forest destruction on (1) the extinction of non-neornithine Avialae and (2) survival patterns among Neornithes must be investigated. Although this hypothesis most likely does not constitute the sole factor influencing end-Cretaceous avian survivorship (indeed, it is unlikely that any single hypothesis completely explains global avian survival patterns), the strength of our results and their compatibility with other studies (e.g., [19, 24]) suggest that selection against avian arboreality across the K-Pg is likely to have played a major role in structuring the early evolutionary history of Neornithes.

Evidence for Global Deforestation at the K-Pg Boundary

The plant fossil record and models of the effects of the Chicxulub impact provide strong evidence for the devastation of forest communities at the K-Pg boundary. Initial disruption came from energy dissipated by the impact blast, leveling trees within a radius of ~1,500 km, and as intense radiated heat, which may have ignited wildfires on a global scale [29–31]. This was most likely followed by acid rain resulting from the emission of sulfate-rich vapor [32] and ejection of a large quantity of soot into the atmosphere [33], potentially blocking photosynthetic activity for several years and most likely inducing limited global climate cooling [34–37]. This phase of suppressed sunlight, notoriously difficult to reconstruct, is supported by the proliferation of saprotrophs thriving on decomposing organic matter [38].

The post-impact recovery of terrestrial plant communities occurred in two phases. The first is marked by the dominance of fern spores in an ~1-cm-thick interval [39] (Figure 3). Ferns are pioneer re-colonizers of devastated landscapes, and their proliferation represents a classic example of a "disaster flora"

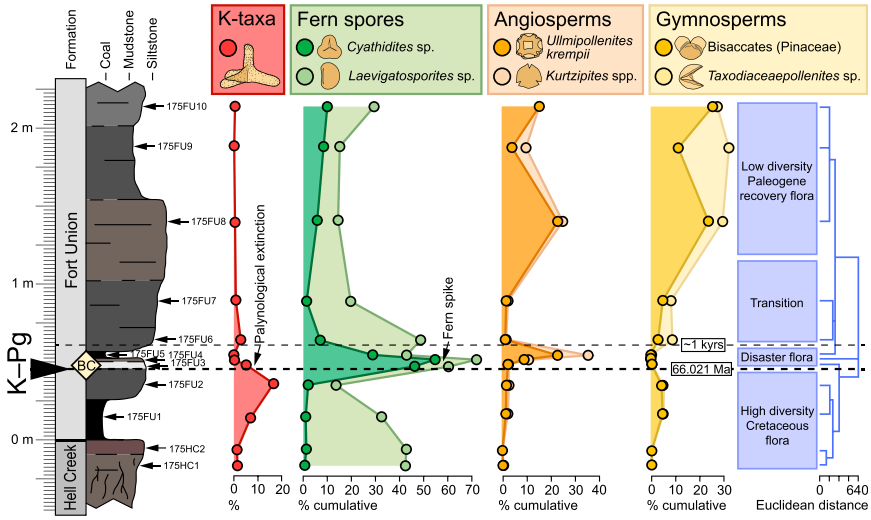

Figure 3. Palynological Record of the John's Nose Section in North Dakota

Extinction (disappearance of K-taxa) and floral turnover are evidenced by changes in relative abundance of common pollen taxa across the K-Pg boundary (modified from [16]). BC, K-Pg boundary clay. See also Figure S1 and Table S1.

composed of taxa capable of rapidly germinating from spores and rhizomes and/or roots. Recent examples of fern spikes have been recorded in the recolonization of rapidly denuded landscapes, such as freshly deposited lava flows in Hawaii, slopes left barren by massive landslides induced by the 1980 eruption of Mount St. Helens, and the short-lived dominance of ferns in the Krakatau floras after its 1883 eruption [8]. The K-Pg fern spike has been identified worldwide and is an indicator of global canopy loss ([14] and references therein). Sedimentation rates based on recent high-resolution radiometric dating of K-Pg bentonites from Montana [40] and the Denver Basin [15] show that establishment of the fern spike occurred within a century of the Chicxulub impact and that the fern spike disaster flora persisted on the order of 1,000 years. This general timescale is corroborated by estimated sedimentation rates from New Zealand (Figure S1). Terrestrial floras were most likely devoid of extensive closed-canopy forests during this phase.

The second phase is marked by the re-establishment of canopy vegetation: the earliest Paleocene marks a change in forest community structure compared to the Cretaceous. Typical earliest Paleocene plant assemblages are characterized by low taxonomic diversity [41–43] and by a shift of dominance toward new angiosperms and conifers (the disappearance of diverse Cretaceous taxa [K-taxa] and proliferation of *Ulmipollenites krempii*, *Kurtzipites* spp., palms [*Arecipites* spp.], *Taxodiaceae*, and *Pinaceae*; Figure 3), long-lived plants that are indicative of modern climax communities [14, 44]. This low-diversity flora persists until the appearance of diversity hotspots ~1.4 Ma after the K-Pg [45].

Today, avian community diversity is negatively influenced by loss of plant diversity and habitat due to human activity, including monospecific agriculture and land-use patterns [46], and the early-Paleocene low-diversity floral phase may have similarly affected avian communities at that time.

Selective extinction of Arboreal Stem Birds at the K-Pg Boundary

As many as five major clades of Mesozoic non-crown avialans are known to have persisted into the final 300,000 years of the Cretaceous [4] and are inferred to have exhibited a diversity of lifestyles (Figure 4). The most diverse and globally widespread of these clades, Enantiornithes, generally exhibit feet with specializations for grasping, including long and opposable hind toes (e.g., [6, 7]). These features have long been used to identify most enantiornithines as tree-dwelling birds [5], although some enantiornithines (e.g., the Late Cretaceous taxa *Elsornis keni* and *Lectavis bretincola*) may have had reduced flight capabilities or wading specializations, suggesting a breadth of ecological habits, including predominantly non-arboreal lifestyles [47]. Other crownward avialans known from the terminal Maastrichtian, such as hesperornithines and ichthyornithines [4, 48], exhibit aquatic ecologies, and the extinction of at least their marine representatives is most likely related to concomitant extinctions among marine tetrapods at the K-Pg boundary [49]. Little is known regarding the ecological habits of Palintropiformes, another clade of near-crown stem birds thought to have persisted up to the K-Pg boundary [4]. If the generally arboreal habits inferred for most Enantiornithes [5] indicate that they were largely associated with forested environments and dependent upon arboreal habitats, then the widespread destruction of forests coincident with the K-Pg transition would undoubtedly have played a major, if not absolute, role in the demise of this dominant Mesozoic clade. The same should be true for any as-yet-undiscovered arboreal specialists among early crown birds and stem-group ornithurines in the late Maastrichtian. More generally, a model of deforestation-related ecological selectivity across the K-Pg boundary may help explain broad-scale patterns in the early evolutionary history of other major vertebrate clades (e.g., [50]).

Selective Survival of Non-arboreal Crown Birds at the K-Pg Boundary

Ancestral state reconstructions for the deepest nodes among crown birds yield a clear signal of ecological selectivity across the K-Pg boundary (Figure 1). The deepest nodes within the bird crown (the most recent common ancestor [MRCA] of Neornithes, Palaeognathae, Neognathae, Galloanserae, and Neoaves) are unambiguously reconstructed as predominantly non-arboreal (Bayesian posterior probabilities and marginal ancestral states all = 100% across both backbone topologies). This reconstruction suggests that no lineages of arboreal crown birds crossed the K-Pg boundary and that the numerous independent transitions toward arboreality across the neornithine tree of life—including ancient transitions within major clades such as Strisores (hummingbirds, nightjars, and kin), Otidimorphae, Columbimorphae (pigeons and kin), and Inopinaves—took place

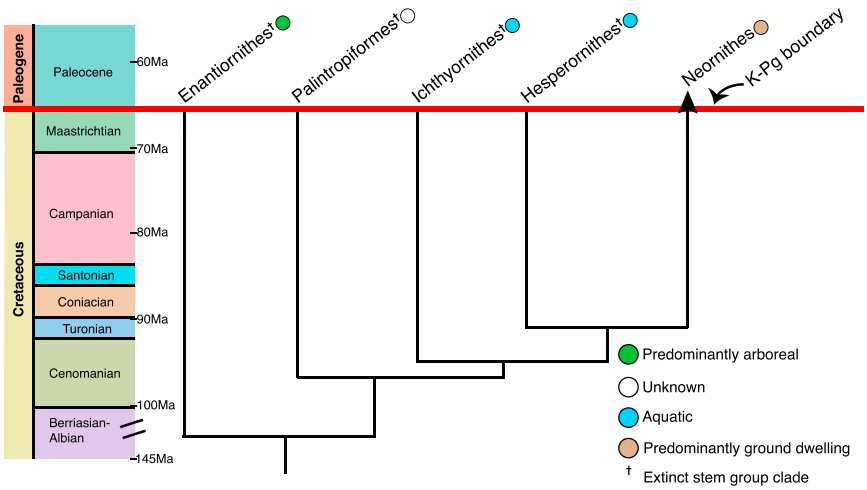

Figure 4. Avialan Diversity at the End-Cretaceous

At least four major clades of near-crown stem neornithines persisted into the latest Maastrichtian [4], including Enantiornithes, the most widespread and diverse clade of Mesozoic Avialae. The figure follows stratigraphic ranges from [4], with topology following recent work (e.g., [21, 22]).

subsequent to the K-Pg transition, presumably after global forests had rebounded from their devastation following the asteroid impact.

Evidence from the Early-Cenozoic Neornithine Fossil Record

The early crown bird fossil record reveals additional support for a survivorship model whereby lineages surviving the K-Pg mass extinction were predominantly ground dwelling. For example, Otidimorphae (one of the most deeply diverging clades within Neoaves [2]) comprises a disparate group of extant birds across three major subclades: turacos (Musophagidae), cuckoos (Cuculidae), and bustards (Otididae) [2] (Figure 2). Extant turacos are medium-sized, predominantly arboreal frugivores, and bustards are large to very large obligate ground dwellers. Cuckoos exhibit more varied ecologies, ranging from predominant ground dwelling in the ''ground cuckoo'' clade Neomorphinae (which includes the greater roadrunner, *Geococcyx californianus*) to predominant arboreality in other subclades [51]. Although the early fossil record of Otidimorphae is sparse [23], the earliest known apparent crown otidimorph is the stem-group turaco, *Foro panarium*, from the early Eocene of Wyoming (D.J.F., unpublished data). Hindlimb proportions covary closely with ecology in Otidimorphae (Figure 2; as they do in many living birds [52]), with arboreal taxa such as turacos and arboreal cuckoos exhibiting relatively short hindlimbs and predominantly ground-dwelling taxa such as neomorphine ground cuckoos and bustards exhibiting long hindlimbs (D.J.F., unpublished data). The long hindlimb proportions of *F. panarium*, which fall within the range of small bustards, suggest that the arboreal habits of crown turacos arose from ground-dwelling ancestors, consistent with a model in which representatives of Neoaves in the early Cenozoic retained the ground-dwelling habits of K-Pg survivors.

The earliest well-constrained neoavian fossil, *Tsidiiyazhi abini*, was recently described from the early Paleocene (~62.5 Ma) of New Mexico [3]. *T. abini* was inferred to represent an early stem mousebird (Coliiformes), a clade exhibiting predominantly arboreal habits today. However, ancestral state reconstructions that include *T. abini* and other early-Cenozoic fossils suggest that hindlimb modifications for perching may have arisen independently in numerous arboreal clades of Telluraves, including Coliiformes, after the K-Pg mass extinction [3]. This evidence supports a model whereby early ground-dwelling neoavians repeatedly took to the trees relatively early in the Paleocene—potentially filling arboreal niches vacated by Cretaceous enantiornithines and stem ornithurines—following the recovery of global forests after the Chicxulub impact.

Conclusions

The sudden onset of the K-Pg extinction event 66.02 Ma poses significant challenges for researchers seeking to unravel its drivers (beyond the asteroid impact itself) and their consequences. These challenges are magnified for taxa with sparse K-Pg fossil records, such as birds, and for scenarios involving phenomena predicted to have taken place over ecological time intervals, such as transient yet widespread impact-related deforestation. Our picture of the contours of this extinction in terms of bird evolutionary history is still incipient; however, consilient evidence from the fossil record [3, 4, 13, 23], molecular divergence time estimates [1, 2, 11], rates of molecular evolution [19], and environmental/ecological reconstructions ([24] and this study) increasingly point to the K-Pg impact and its consequences as playing major roles in the selective filtering of bird survivorship. All available evidence appears congruent with the globally widespread destruction of forests coincident with the K-Pg event imposing a strict filter against the persistence of avialans exhibiting arboreal ecologies.

A succession of events implicated in the destruction of global forests would have primarily affected arboreal taxa, including shockwaves knocking down trees immediately after the impact, wild fires directly eliminating forest habitats, and reduced light levels and associated global cooling delaying forest recovery. Although a multitude of factors undoubtedly influenced avian evolution at the end-Cretaceous mass extinction, including diet [24, 28], body size [19], breeding habits [27], and flight capacity [53], selection for non-arboreal habits appears to have left an indelible mark on the early evolutionary history of crown birds, clearly discernible more than 66 million years later.

STAR★METHODS

Detailed methods are provided in the online version of this paper and include the following:

- KEY RESOURCES TABLE
- CONTACT FOR REAGENT AND RESOURCE SHARING

SUPPLEMENTAL INFORMATION

Supplemental Information includes four figures and two tables and can be found with this article online at https://doi.org/10.1016/j.cub.2018.04.062.

ACKNOWLEDGMENTS

We thank S. Wing, A. Goswami, R. Prum, A. Heers, and A. Chen for thoughtful discussion and D.A. Pearson and M. Clark for logistical support and assistance in the field. D.J.F. is supported by a 50th Anniversary Prize Fellowship at the University of Bath. A.B. acknowledges support from the Smithsonian NMNH Deep Time Peter Buck Postdoctoral Fellowship. V.V. was supported by Swedish Research Council VR grant 2015-4264. J.S.B. was supported by NSF grants DGE-1650441 and DEB-1700786. J.A.G. thanks the Yale Peabody Museum of Natural History. This is contribution 381 from the Smithsonian NMNH ETE consortium.

AUTHOR CONTRIBUTIONS

Conceptualization, D.J.F. and J.A.G.; Methodology, D.J.F., A.B., J.S.B., R.D., T.R.L., and V.V.; Investigation, D.J.F., A.B., J.S.B., and V.V.; Writing – Original Draft, D.J.F.; Writing – Review and Editing, D.J.F., A.B., J.S.B., R.D., D.E.F., T.R.L., V.V., and J.A.G.

DECLARATION OF INTERESTS

The authors declare no competing interests.

Received: February 27, 2018
Revised: March 19, 2018
Accepted: April 18, 2018
Published: May 24, 2018

REFERENCES

1. Jarvis, E.D., Mirarab, S., Aberer, A.J., Li, B., Houde, P., Li, C., Ho, S.Y.W., Faircloth, B.C., Nabholz, B., Howard, J.T., et al. (2014). Whole-genome analyses resolve early branches in the tree of life of modern birds. Science *346*, 1320–1331.
2. Prum, R.O., Berv, J.S., Dornburg, A., Field, D.J., Townsend, J.P., Lemmon, E.M., and Lemmon, A.R. (2015). A comprehensive phylogeny of birds (Aves) using targeted next-generation DNA sequencing. Nature *526*, 569–573.
3. Ksepka, D.T., Stidham, T.A., and Williamson, T.E. (2017). Early Paleocene landbird supports rapid phylogenetic and morphological diversification of crown birds after the K-Pg mass extinction. Proc. Natl. Acad. Sci. USA *114*, 8047–8052.
4. Longrich, N.R., Tokaryk, T., and Field, D.J. (2011). Mass extinction of birds at the Cretaceous-Paleogene (K-Pg) boundary. Proc. Natl. Acad. Sci. USA *108*, 15253–15257.
5. Chiappe, L.M., and Qingjin, M. (2016). Birds of Stone: Chinese Avian Fossils from the Age of Dinosaurs (JHU Press).
6. Hopson, J.A. (2001). Ecomorphology of avian and nonavian theropod phalangeal proportions: Implications for the arboreal versus terrestrial origin of bird flight. In New Perspectives on the Origin and Early Evolution of Birds, J.A. Gauthier, and L.F. Gall, eds. (Yale University Peabody Museum), pp. 211–235.
7. O'Connor, J.K., Chiappe, L.M., Gao, C., and Zhao, B. (2011). Anatomy of the Early Cretaceous enantiornithine bird Rapaxavis pani. Acta Palaeontol. Pol. *56*, 463–475.
8. Tschudy, R.H., Pillmore, C.L., Orth, C.J., Gilmore, J.S., and Knight, J.D. (1984). Disruption of the terrestrial plant ecosystem at the Cretaceous-Tertiary boundary, Western interior. Science *225*, 1030–1032.
9. Vajda, V., Raine, J.I., and Hollis, C.J. (2001). Indication of global deforestation at the Cretaceous-Tertiary boundary by New Zealand fern spike. Science *294*, 1700–1702.
10. Gauthier, J. (1986). Saurischian monophyly and the origin of birds. Memoirs of the California Academy of Sciences *8*, 1–55.
11. Claramunt, S., and Cracraft, J. (2015). A new time tree reveals Earth history's imprint on the evolution of modern birds. Sci. Adv. *1*, e1501005.
12. Reddy, S., Kimball, R.T., Pandey, A., Hosner, P.A., Braun, M.J., Hackett, S.J., Han, K.-L., Harshman, J., Huddleston, C.J., Kingston, S., et al. (2017). Why do phylogenomic data sets yield conflicting trees? Data type influences the avian tree of life more than taxon sampling. Syst. Biol. *66*, 857–879.
13. Field, D.J. (2017). Big-time insights from a tiny bird fossil. Proc. Natl. Acad. Sci. USA *114*, 7750–7752.
14. Vajda, V., and Bercovici, A. (2014). The global vegetation pattern across the Cretaceous–Paleogene mass extinction interval: a template for other extinction events. Global Planet. Change *122*, 29–49.
15. Clyde, W.C., Ramezani, J., Johnson, K.R., Bowring, S.A., and Jones, M.M. (2016). Direct high-precision U–Pb geochronology of the end-Cretaceous extinction and calibration of Paleocene astronomical timescales. Earth Planet. Sci. Lett. *452*, 272–280.
16. Bercovici, A., Vajda, V., Pearson, D., Villanueva-Amadoz, U., and Kline, D. (2012). Palynostratigraphy of John's Nose, a new Cretaceous—Paleogene boundary section in southwestern North Dakota, USA. Palynology *36*, 36–47.
17. Fastovsky, D.E., and Bercovici, A. (2016). The Hell Creek Formation and its contribution to the Cretaceous–Paleogene extinction: a short primer. Cretac. Res. *57*, 368–390.
18. Feduccia, A. (1995). Explosive evolution in tertiary birds and mammals. Science *267*, 637–638.
19. Berv, J.S., and Field, D.J. (2018). Genomic Signature of an Avian Lilliput Effect across the K-Pg Extinction. Syst. Biol. *67*, 1–13.
20. Brusatte, S.L., Butler, R.J., Barrett, P.M., Carrano, M.T., Evans, D.C., Lloyd, G.T., Mannion, P.D., Norell, M.A., Peppe, D.J., Upchurch, P., and Williamson, T.E. (2015). The extinction of the dinosaurs. Biol. Rev. Camb. Philos. Soc. *90*, 628–642.
21. Field, D.J., Hanson, M., Burnham, D.A., Wilson, L.E., Super, K., Ehret, D.J., Ebersole, J.A., and Bhullar, B.A.S. (2018). Complete *Ichthyornis* skull illuminates mosaic assembly of the avian head. Nature *557*, 96–100.
22. Bell, A., and Chiappe, L.M. (2016). A species-level phylogeny of the Cretaceous Hesperornithiformes (Aves: Ornithuromorpha): implications for body size evolution amongst the earliest diving birds. J. Syst. Palaeontology *14*, 239–251.
23. Mayr, G. (2009). Paleogene Fossil Birds (Springer).
24. Larson, D.W., Brown, C.M., and Evans, D.C. (2016). Dental disparity and ecological stability in bird-like dinosaurs prior to the end-Cretaceous mass extinction. Curr. Biol. *26*, 1325–1333.
25. Zhou, Z., and Zhang, F. (2002). A long-tailed, seed-eating bird from the Early Cretaceous of China. Nature *418*, 405–409.
26. Louchart, A., and Viriot, L. (2011). From snout to beak: the loss of teeth in birds. Trends Ecol. Evol. *26*, 663–673.
27. Varricchio, D.J., and Jackson, F.D. (2016). Reproduction in Mesozoic birds and evolution of the modern avian reproductive mode. Auk *133*, 654–684.

28. O'Connor, J., Wang, X., Sullivan, C., Wang, Y., Zheng, X., Hu, H., Zhang, X., and Zhou, Z. (2018). First report of gastroliths in the Early Cretaceous basal bird Jeholornis. Cretac. Res. *84*, 200–208.
29. Wolbach, W.S., Gilmour, I., Anders, E., Orth, C.J., and Brooks, R.R. (1988). Global fire at the Cretaceous–Tertiary boundary. Nature *334*, 665–669.
30. Anders, E., Wolbach, W.S., and Gilmour, I. (1991). Major Wildfires at the Cretaceous-Tertiary Boundary. In Global Biomass Burning: Atmospheric, Climatic and Biospheric Implications, J.S. Levine, ed. (MIT Press), pp. 485–492.
31. Robertson, D.S., Lewis, W.M., Sheehan, P.M., and Toon, O.B. (2013). K-Pg extinction: reevaluation of the heat-fire hypothesis. J. Geophys. Res. Biogeosci. *118*, 329–336.
32. Ohno, S., Kadono, T., Kurosawa, K., Hamura, T., Sakaiya, T., Shigemori, K., Hironaka, Y., Sano, T., Watari, T., and Otani, K. (2014). Production of sulphate-rich vapour during the Chicxulub impact and implications for ocean acidification. Nat. Geosci. *7*, 279–282.
33. Kaiho, K., Oshima, N., Adachi, K., Adachi, Y., Mizukami, T., Fujibayashi, M., and Saito, R. (2016). Global climate change driven by soot at the K-Pg boundary as the cause of the mass extinction. Sci. Rep. *6*, 28427.
34. Vellekoop, J., Esmeray-Senlet, S., Miller, K.G., Browning, J.V., Sluijs, A., van de Schootbrugge, B., Damsté, J.S.S., and Brinkhuis, H. (2016). Evidence for Cretaceous-Paleogene boundary bolide "impact winter" conditions from New Jersey, USA. Geology *44*, 619–622.
35. Bardeen, C.G., Garcia, R.R., Toon, O.B., and Conley, A.J. (2017). On transient climate change at the Cretaceous-Paleogene boundary due to atmospheric soot injections. Proc. Natl. Acad. Sci. USA *114*, E7415–E7424.
36. Brugger, J., Feulner, G., and Petri, S. (2017). Baby, it's cold outside: climate model simulations of the effects of the asteroid impact at the end of the Cretaceous. Geophys. Res. Lett. *44*, 419–427.
37. Vajda, V., Ocampo, A., Ferrow, E., and Koch, C.B. (2015). Nano particles as the primary cause for long-term sunlight suppression at high southern latitudes following the Chicxulub impact—evidence from ejecta deposits in Belize and Mexico. Gondwana Res. *27*, 1079–1088.
38. Vajda, V., and McLoughlin, S. (2004). Fungal proliferation at the Cretaceous-Tertiary boundary. Science *303*, 1489.
39. Wolfe, J.A., and Upchurch, G.R., Jr. (1986). Vegetation, climatic and floral changes at the Cretaceous-Tertiary boundary. Nature *324*, 148.
40. Renne, P.R., Deino, A.L., Hilgen, F.J., Kuiper, K.F., Mark, D.F., Mitchell, W.S., 3rd, Morgan, L.E., Mundil, R., and Smit, J. (2013). Time scales of critical events around the Cretaceous-Paleogene boundary. Science *339*, 684–687.
41. Johnson, K.R. (1992). Leaf-fossil evidence for extensive floral extinction at the Cretaceous-Tertiary boundary, North Dakota, USA. Cretac. Res. *13*, 91–117.
42. Johnson, K.R. (2002). Megaflora of the Hell Creek and lower Fort Union Formations in the western Dakotas: vegetational response to climate change, the Cretaceous-Tertiary boundary event, and rapid marine transgression. Spec. Pap. Geol. Soc. Am. *361*, 329–391.
43. Bercovici, A., Jacqueline, W., and Pearson, D. (2008). Detailed palaeontologic and taphonomic techniques to reconstruct an earliest Paleocene fossil flora: an example from southwestern North Dakota, USA. Rev. Palaeobot. Palynol. *151*, 136–146.
44. Vajda, V., and McLoughlin, S. (2007). Extinction and recovery patterns of the vegetation across the Cretaceous–Palaeogene boundary—a tool for unravelling the causes of the end-Permian mass-extinction. Rev. Palaeobot. Palynol. *144*, 99–112.
45. Johnson, K.R., and Ellis, B. (2002). A tropical rainforest in Colorado 1.4 million years after the Cretaceous-Tertiary boundary. Science *296*, 2379–2383.
46. Lee, M.-B., and Martin, J.A. (2017). Avian species and functional diversity in agricultural landscapes: does landscape heterogeneity matter? PLoS ONE *12*, e0170540.
47. Chiappe, L.M., and Walker, C.A. (2002). Skeletal morphology and systematics of the Cretaceous Euenantiornithes (Ornithothoraces: Enantiornithes). In Mesozoic Birds: Above the Heads of Dinosaurs, L.M. Chiappe, and L.M. Witmer, eds. (University of California Press), pp. 240–267.
48. Dumont, M., Tafforeau, P., Bertin, T., Bhullar, B.-A., Field, D., Schulp, A., Strilisky, B., Thivichon-Prince, B., Viriot, L., and Louchart, A. (2016). Synchrotron imaging of dentition provides insights into the biology of Hesperornis and Ichthyornis, the "last" toothed birds. BMC Evol. Biol. *16*, 178.
49. Schulte, P., Alegret, L., Arenillas, I., Arz, J.A., Barton, P.J., Bown, P.R., Bralower, T.J., Christeson, G.L., Claeys, P., Cockell, C.S., et al. (2010). The Chicxulub asteroid impact and mass extinction at the Cretaceous-Paleogene boundary. Science *327*, 1214–1218.
50. Feng, Y.-J., Blackburn, D.C., Liang, D., Hillis, D.M., Wake, D.B., Cannatella, D.C., and Zhang, P. (2017). Phylogenomics reveals rapid, simultaneous diversification of three major clades of Gondwanan frogs at the Cretaceous-Paleogene boundary. Proc. Natl. Acad. Sci. USA *114*, E5864–E5870.
51. Payne, R.B. (1997). Family Cuculidae (cuckoos). In Handbook of the Birds of the World, Volume 4, Sandgrouse to Cuckoos, J. del Hoyo, A. Elliott, and J. Sargatal, eds. (Lynx Edicions), pp. 508–607.
52. Norberg, U.M. (1979). Morphology of the wings, legs and tail of three coniferous forest tits, the goldcrest, and the treecreeper in relation to locomotor pattern and feeding station selection. Philos. Trans. R. Soc. Lond. B Biol. Sci. *287*, 131–165.
53. Feo, T.J., Field, D.J., and Prum, R.O. (2015). Barb geometry of asymmetrical feathers reveals a transitional morphology in the evolution of avian flight. Proc. Biol. Sci. *282*, 20142864.
54. Ocampo, A., Vajda, V., and Buffetaut, E. (2006). Unravelling the Cretaceous-Paleogene (KT) catastrophe: evidence from flora fauna and geology. In Biological Processes Associated with Impact Events, C. Cockell, I. Gilmour, and C. Koeberl, eds. (Springer), pp. 203–227.
55. Del Hoyo, J., Elliot, A., and Sargatal, J. (1992). Handbook of the Birds of the World (Lynx Editions).
56. Hsiang, A.Y., Field, D.J., Webster, T.H., Behlke, A.D.B., Davis, M.B., Racicot, R.A., and Gauthier, J.A. (2015). The origin of snakes: revealing the ecology, behavior, and evolutionary history of early snakes using genomics, phenomics, and the fossil record. BMC Evol. Biol. *15*, 87.
57. Olson, S.L. (1992). A new family of primitive landbirds from the Lower Eocene Green River Formation of Wyoming. In Papers in Avian Paleontology Honoring Pierce Brodkorb, *Volume 36*, K.E. Campbell, ed. (Natural History Museum of Los Angeles County), pp. 137–160.
58. Team, R.D.C. (2003). R: a language and environment for statistical computing (R Foundation for Statistical Computing).
59. Paradis, E., Claude, J., and Strimmer, K. (2004). APE: analyses of phylogenetics and evolution in R language. Bioinformatics *20*, 289–290.
60. Revell, L.J. (2012). Phytools: an R package for phylogenetic comparative biology (and other things). Methods Ecol. Evol. *3*, 217–223.
61. Bollback, J.P. (2006). SIMMAP: stochastic character mapping of discrete traits on phylogenies. BMC Bioinformatics *7*, 88.
62. Schliep, K.P. (2011). phangorn: phylogenetic analysis in R. Bioinformatics *27*, 592–593.

STAR★METHODS

KEY RESOURCES TABLE

REAGENT or RESOURCE	SOURCE	IDENTIFIER
Deposited Data		
Scripts for AERs, all input data, and all AER results	This paper	http://doi.org/10.5281/zenodo.1204464

CONTACT FOR REAGENT AND RESOURCE SHARING

Further information and requests for resources and reagents should be directed to and will be fulfilled by the Lead Contact, Daniel J. Field (d.j.field@bath.ac.uk).

METHOD DETAILS

Examining the extent of end-Cretaceous deforestation

Floral changes were characterized by analyzing relative abundance data of palynomorphs (pollen, spores, algae) from twelve samples spanning the K–Pg boundary from the John's Nose section, southwest North Dakota [16]. Stages of recovery were categorized based on Euclidean Distance of the relative abundance data for the 12 palynological assemblages. Raw abundance data and stratigraphic sampling resolution are presented in Table S1.

Determining the approximate time frame of K–Pg forest recovery

The onset of fern recovery is estimated based on Iridium content in the sediments hosting the fern-spore spike based on the fall-out time calculated in Ocampo et al. [54]. The duration of fern spore dominance is based on combined calculations of sedimentation rates from K-Pg boundary successions in New Zealand [9] and the USA [15].

Neornithine ancestral ecological reconstructions

Ancestral ecological reconstructions (AERs) were performed using recent time-scaled neornithine phylogenies incorporating nearly every extant avian family-level clade [2, 11]. The 198 extant species in the original Prum et al. phylogenetic dataset [2], and the 229 from Claramunt and Cracraft [11] were scored as either predominantly arboreal, predominantly non-arboreal, or 'mixed' (for taxa that spend much of their time in both arboreal and non-arboreal settings). These alternative hypotheses span the present range of uncertainty with regard to neornithine phylogenetic topology and divergence times. Scorings were based on descriptions of general ecology, nest substrate, and foraging substrate from [55]. Discrete codings for general lifestyle and nest substrate categories are presented at http://doi.org/10.5281/zenodo.1204464, along with annotated R code (to reproduce all analyses) and alternative reconstructions. Categorizing behavior for the purpose of ancestral ecological reconstructions can be subjective (e.g., [56]); however, we consider our criteria for bounding categories to be consistent, and to capture the predominant ecological habits of each included species. For example, while the Greater Roadrunner (*Geococcyx californianus*) is known to nest in low trees and bushes between 1-3 m above the ground [55], it is generally considered predominantly ground-dwelling (a scoring that well-reflects its general lifestyle and foraging substrate), and we therefore considered 'non-arboreal' to be a more suitable category for *G. californianus* than 'mixed'. We believe that our conclusions are robust to alternative codings in similar borderline cases, such as the Shining-blue Kingfisher (*Alcedo quadribrachys*), which nests in burrows but is otherwise well classified as tree-dwelling and was therefore classified as generally arboreal. Additionally, we performed reconstructions using scores for general nest category (nests in trees versus nests on ground versus nests either in trees or on ground), codings that may be less subjective. These reconstructions unambiguously support ground-nesting habits as ancestral for the deepest neornithine nodes. The scenario supported by these results (clear bias toward non-arboreal nesting across the K–Pg) is qualitatively the same as that from our analysis of general lifestyle, and so are presented as supporting data (Figure S2 and http://doi.org/10.5281/zenodo.1204464).

Fossil bird ecomorphology

An existing morphometric dataset for Otidimorphae (D.J.F., unpublished data) was expanded. Digital calipers sensitive to 0.01mm were used to measure the total length of the femur, tibiotarsus, and tarsometatarsus for adult turacos, cuckoos, and bustards (raw data in Table S2). Seven species of Musophagidae were examined, representing every major musophagid subclade. Thirty species of Cuculidae were examined from across the extant diversity of cuckoos, and five species of Otididae were measured. Following (D.J.F., unpublished data), measurements from extant taxa were compared to measurements from the fossil stem turaco *Foro panarium* (D.J.F., unpublished data; [57]).

QUANTIFICATION AND STATISTICAL ANALYSIS

Ancestral ecological reconstructions

Likelihood-based AERs were performed in R [58] using the ace() likelihood function in ape [59] and the make.simmap() Bayesian stochastic character mapping (SIMMAP) function in phytools [60, 61]. For both sets of analyses, we implemented a two-rate transition matrix that defines one rate for forward and reverse transitions between arboreality and non-arboreality, and another rate for forward and reverse transitions between mixed and arboreal states, and mixed and non-arboreal states (in *R:* matrix(c(0, 2, 1, 2, 0, 2, 1, 2, 0), nrow = 3)). This model allows transitions that pass through the mixed phase to be favored, without preventing direct transitions. Under this model, the marginal ancestral states (from ace) and Bayesian posterior probabilities from SIMMAP were nearly identical ($R^2 > 0.99$), so we present our Bayesian results in Figure 1, summarized across 1,000 stochastic character maps. Predominant arboreality and predominant non-arboreality dominated inferred reconstructions throughout the tree (41.8% and 50.5% of the tree, respectively), with mixed ecologies reconstructed across only 7.7% of the tree in Figure 1. We also performed maximum parsimony reconstructions of ancestral ecological habits and nesting substrate using the ancestral.pars() function with regular MPR optimization implemented in the phangorn *R* package [62] (Figure S3 and http://doi.org/10.5281/zenodo.1204464), which corroborated the results described above.

Fossil bird ecomorphology

Following (D.J.F., unpublished data), hindlimb indices were calculated by summing the lengths of the tarsometatarsus and tibiotarsus, and dividing by the length of the femur.

DATA AND SOFTWARE AVAILABILITY

Scripts for the ancestral ecological reconstructions, as well as the input data for these analyses and all AER results are archived at http://doi.org/10.5281/zenodo.1204464.

Current Biology, Volume *28*

Supplemental Information

Early Evolution of Modern Birds Structured by Global Forest Collapse at the End-Cretaceous Mass Extinction

Daniel J. Field, Antoine Bercovici, Jacob S. Berv, Regan Dunn, David E. Fastovsky, Tyler R. Lyson, Vivi Vajda, and Jacques A. Gauthier

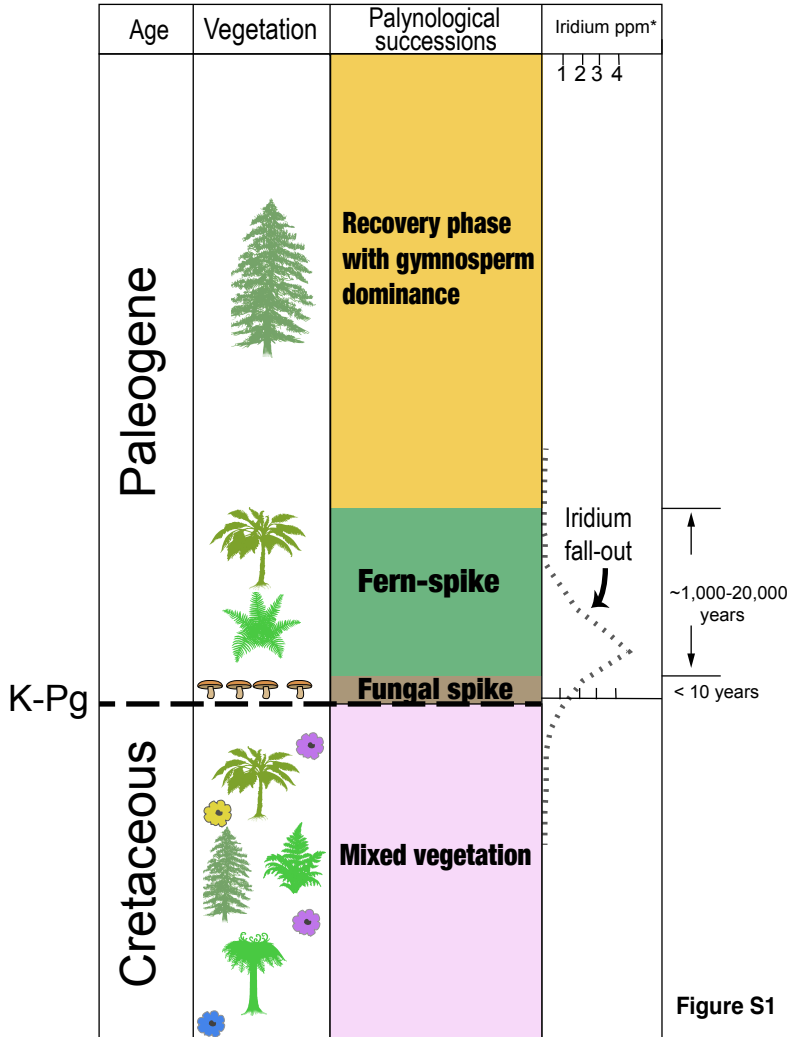
Age
Vegetation
Palynological successions
Iridium ppm*
1 2 3 4
Paleogene
Recovery phase with gymnosperm dominance
Fern-spike
Fungal spike
Iridium fall-out
~1,000-20,000 years
< 10 years
K-Pg
Cretaceous
Mixed vegetation

Figure S1

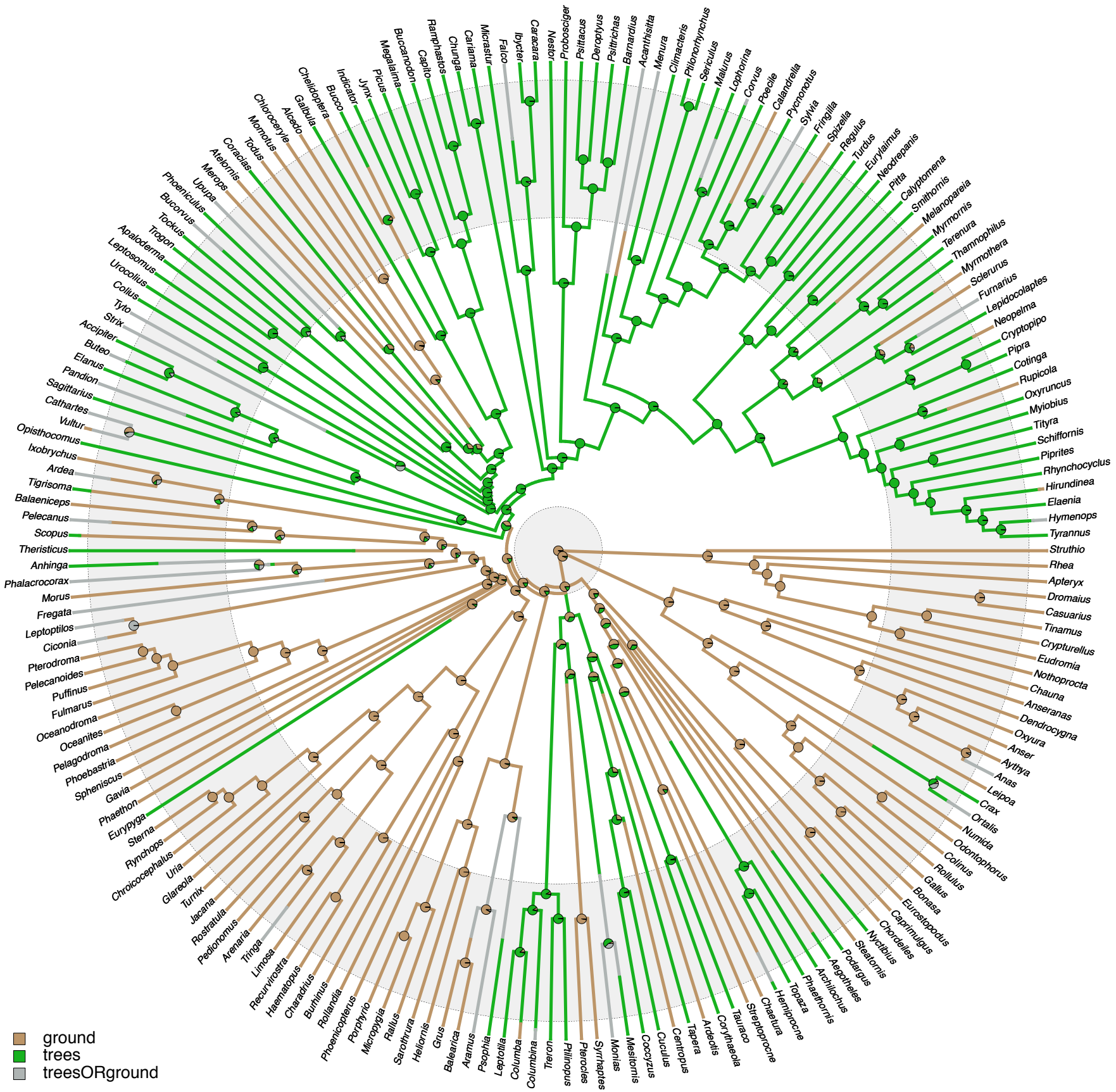

Figure S2


Consistency Index = 0.083
Retention Index = 0.636
steps = 36
arboreal
mixed
nonarboreal

Figure S3

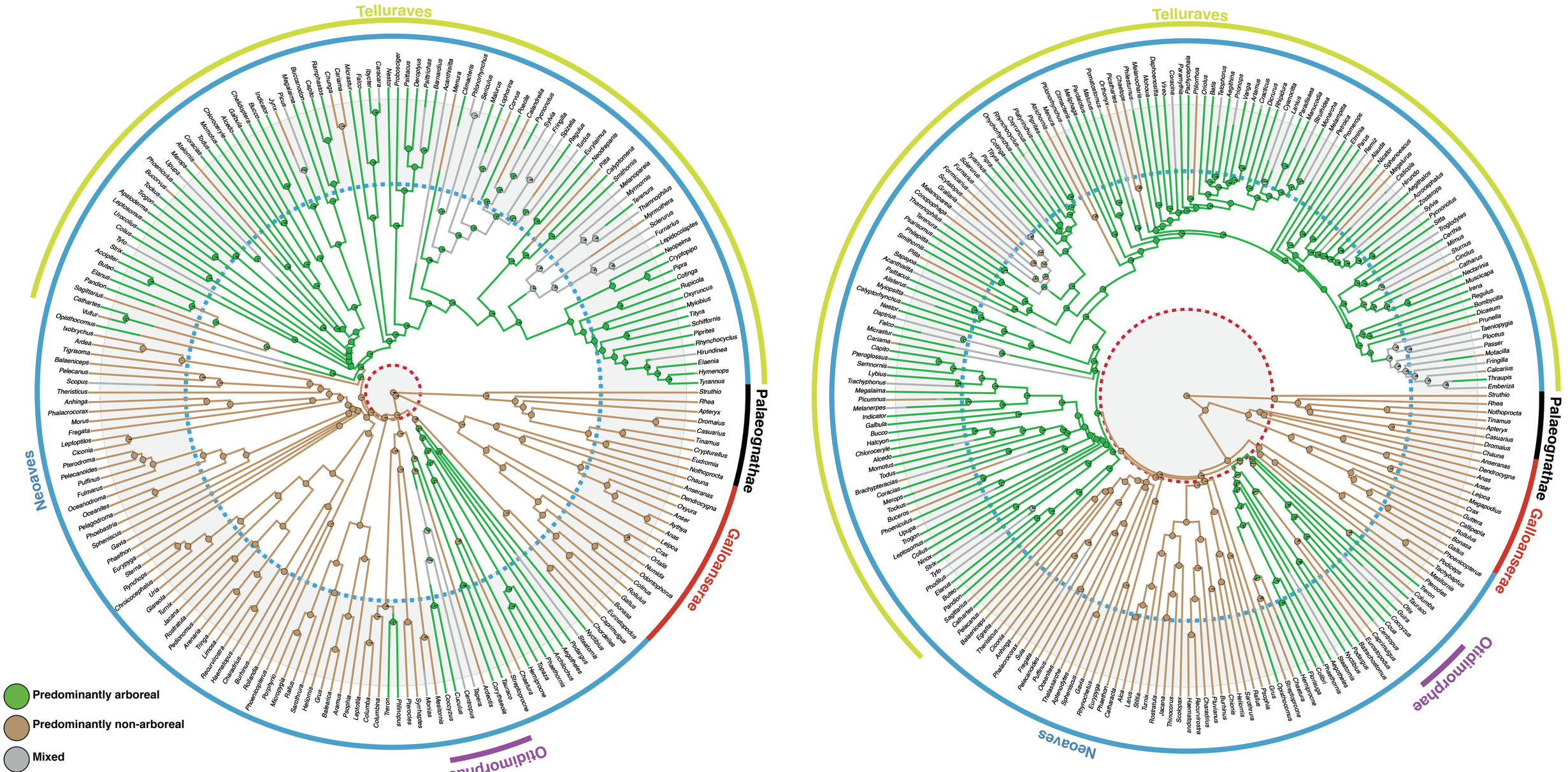
Telluraves
Neoaves
Palaeognathae
Gallonserae
Otidimorphae
Predominantly arboreal
Predominantly non-arboreal
Mixed

Figure S4

Figure S1

Schematic illustration of floral extinction and recovery phases across the K–Pg boundary. Related to Figure 3. Correlated between northern and southern hemisphere successions (i.e. USA and New Zealand) compared to Iridium abundance data from Vajda et al. [S1]. The fern spike was initiated within a few years following the impact based on modeling [S2] and identification of Fe-nanoparticles in the K–Pg boundary ejecta layer in Mexico and New Zealand [S3, S4]. The rapid initial recovery of photosynthetic plants is traceable in the Moody Creek Mine succession where the fern abundance is identified in carbonaceous siltstones also illustrating high levels of Iridium [S5], indicating that Iridium was still falling out from the atmosphere as light-levels normalized and plant recovery initiated. The timeframe for the fern-dominated interval is based on K–Pg boundary succession sedimentation rates from New Zealand [S1] and the USA [S6]. Calculations based on New Zealand marine successions yield estimates of 8,000-20,000 years, within the range estimated for successions from the US western interior [S6].

Figure S2

Ancestral ecological reconstructions reveal bias toward ground nesting birds across the K–Pg. Related to Figure 1. Bayesian and likelihood ancestral ecological reconstructions (AER) using the topology illustrated in Figure 1 [S7] show that at least the six most deeply diverging crown bird clades, including Neornithes (all crown birds), Neognathae (Galloanserae + Neoaves), and Neoaves, are reconstructed as ancestrally ground nesting (*pp* = 0.94, 0.94, 0.84, 0.84, 0.84, 0.84, respectively), with numerous

independent transitions toward nesting in trees arising in the early Cenozoic, presumably after global forests had recovered from the Chicxulub impact. Concentric background rings demarcate geologic periods: inner grey circle at the center is Late Cretaceous; white ring is the Paleogene (66.02-23.03Ma); outer grey ring is the Neogene (23.03-2.58Ma). Tips extend to the present. Piecharts at nodes indicate SIMMAP posterior probabilities for ancestral nest ecology, under our model. Branch colors represent a single randomly sampled stochastic character map from a posterior sample of 1,000 maps. See doi.org/10.5281/zenodo.1204464 for replicate analysis performed on the alternative backbone topology of Claramunt and Cracraft [S8].

Figure S3

Ancestral ecological reconstructions reveal bias toward non-arboreal birds across the K–Pg. Related to Figure 1. Parsimony reconstruction of the analysis presented in Figure 1.

Figure S4

Comparison of Bayesian SIMMAP AER results for general ecology using the phylogenetic hypotheses of Prum et al. [S7] and Claramunt and Cracraft [S8]. Related to Figure 1.

Prum et al. [S7] topology on the left; Claramunt and Cracraft [S8] on the right. Major clades discussed in the main text are highlighted. Both topologies support the persistence of exclusively non-arboreal neornithines across the K–Pg.

Strat. pos. relative to K–Pg (cm):	175HC1 -60	175HC2 -49	175FU1 -28	175FU2 -7	175FU3 1	175FU4 3	175FU5 5	175FU6 20	175FU7 43	175FU8 97	175FU9 138	175FU10 174
Bryophytes	20,3 %	29,8 %	15,2 %	1,6 %	1,9 %	0,0 %	0,2 %	4,6 %	26,7 %	2,0 %	2,2 %	0,7 %
Foraminisporis undulatus	10	6										
Stereisporites spp.	95	186	79	6	11		1	28	186	12	14	3
Zlivisporites novomexicanum				2								
Quillworts	0,0 %	0,0 %	0,0 %	0,0 %	0,0 %	0,0 %	0,0 %	0,0 %	0,0 %	5,8 %	8,5 %	0,5 %
Palaeoisoetes subengelmanii										34	55	2
Lycopods	5,2 %	3,0 %	0,8 %	0,4 %	0,5 %	0,0 %	0,3 %	0,2 %	0,4 %	0,0 %	0,2 %	0,0 %
Hamulatisporis amplus	1	6	1	1	1		1		2			
Hamulatisporis hamulatis	26	13			1							
Retitriletes sp.			3	1	1		1	1	1		1	
Ferns	63,8 %	57,9 %	52,2 %	27,0 %	69,1 %	83,4 %	51,6 %	70,9 %	43,9 %	22,3 %	25,0 %	42,2 %
Azolla circinata					2	3			5	5	13	
Azolla cretacea				5	3	31	3		1		1	1
Azolla microspore	3		19	3	4	6	9	4	8	1	5	11
Cicatricosisporites spp.	1	4	3		5		1	17	9	1		
Cyathidites spp.	3	8	5	9	273	673	189	43	8	34	56	41
Deltoidospora sp.	44	35	34	25	5	19	8	33	68	6	3	21
Ghoshispora bella				19	2	1			2	1	8	1
Gleicheniidites spp.	14	22	29	20	9		4	45	45	25	23	9
Laevigatosporites spp.	231	287	166	54	85	215	95	269	139	55	47	83
Leptolepidites tenuis	12	1									3	1
Osmundacidites stanleyi		1	2	1	2	1			5		2	1
Polycingulatisporites sp.	16	14										
Reticuloidosporites pseudomurii	1	1	13		8	1	6	17	10	1	1	2
Toroisporis major	4								6	3		
3-12								3				
Gymnosperms	3,5 %	2,6 %	7,9 %	7,1 %	1,9 %	0,9 %	2,1 %	9,7 %	9,5 %	31,1 %	33,2 %	28,9 %
Araucariapollenites sp.										1		
Classopollis sp.												1
Cycadopites spp.	17	15	16	10	6	3	9	7	8	5	6	5
Ephedripites ovatus				1								
Inaperturopollenites spp.				1		6	4					
Bisaccates spp.	1	2	24	20	5	1		18	35	137	73	100
Podocarpidites spp.									1	3	3	2
Taxodiaceaepollenites spp.			1	4				34	22	34	133	8
Tsugapollenites sp.										4		1
Monocotyledon	0,6 %	0,8 %	1,0 %	1,8 %	0,5 %	0,7 %	1,6 %	3,1 %	2,2 %	1,5 %	6,0 %	1,7 %
Arecipites spp.	2			4	3		4	17	10	4	7	5
Dyadonapites reticulatus									1		2	
Liliacidites altimurus										1		
Liliacidites complexus	1		4	3					2			
Pandaniidites typicus			1			2	6	2	1	3	8	2
Penetetrapites sp.		5		2		6			1	1	22	
Dicotyledons	5,8 %	5,9 %	22,2 %	60,1 %	25,0 %	14,0 %	43,4 %	10,9 %	15,1 %	33,0 %	21,9 %	22,7 %
**Aquilapollenites collaris*				7	1			1				
**Aquilapollenites conatus*		1			1							
**Aquilapollenites marmarthensis*			25	22	5	1		13	4			1
**Aquilapollenites mtshedlishvili*	4	2	1	3								
**Aquilapollenites quadricretaeus*				1								
**Aquilapollenites quadrilobus*		4	1	1								
Chenopodipollis sp.	1								1	2		
Discoidites parvistriatus	1	4		2	7		2	1				
Ericaceoipollenites sp.				58	7	2	9	1	4	13	44	1
Eucommidites sp.				8								
Inaperturotetradites scabratus						2	9		1			
Kurtzipites circularis	1		4	5		19	59	1	4	9	37	2
Kurtzipites trispissatus					1	2	18	1	1	3		1
Lanagiopollis lihokus			1									
**Leptopecopites pocockii*				1	2							
**Libopollis jarzeni*	3			1								
Nyssapollenites spp.									1			
Retibrevitricolporites beccus			1	1								
Retitrescolpites anguloluminosus		1			1					1		1
Rhoipites spp.			3							1		1
Simplicepollis rallus				3	2	1		2	1		2	
**Striatellipollis striatellus*				32	20	1		2		1		
Striatopollis tectatus				1	1		1	1		2		
**Styxpollenites calamitas*		1	1									
Tricolpites spp.	2		1	11	5	3	1	2	2	6	4	13
**Tricolpites microreticulatus*				3						1		1
Triporopollenites spp.	2	3	64	131	75	22	25	30	72	19	26	8
**Tschudypollis* spp.		1	3	1	1	1		2			1	
Ullmipollenites krempii	3	2	9	10	15	106	141	9	13	137	28	63
Wodehouseia spinata	13	19	1	1					1			
Algae	0,8 %	0,0 %	0,8 %	2,0 %	1,0 %	1,0 %	0,7 %	0,7 %	2,3 %	1,2 %	0,9 %	0,0 %
Ovoidites sp.						1	3				1	
Pediastrum sp.				1						2	2	
Tetraporina sp.				2	6	4	1	2		3	2	
Tetraguladinium conspicuum												
Schizophacus sp.	2		4	5		6		2	6	2	1	
4-14									2			
4-17				2								
4-22									8			
4-26	2											
Dinoflagellates	0,0 %	0,0 %	0,0 %	0,0 %	0,0 %	0,0 %	0,0 %	0,0 %	0,0 %	3,0 %	2,2 %	3,2 %
Dinoflagellates										18	14	13
Total	516	644	519	504	576	1139	610	608	697	591	648	405

Table S1

Species	Family	Lifestyle	Femur Length (mm)	Tibiotarsus Length (mm)	Tarsometatarsus Length (mm)	Hindlimb Index	% Femur of total hindlimb length	% Tibiotarsus of total hindlimb length	% Tarsometatarsus of total hindlimb length	Lifestyle scorings
Tauraco corythaix	Musophagidae	1	56.43	77.67	45.02	2.174198122	31.50	43.36	25.13	1 tree
Tauraco leucolophus	Musophagidae	1	49.70	69.05	38.51	2.164185111	31.60	43.91	24.49	2 ground
Tauraco schalowi	Musophagidae	1	52.13	72.04	40.28	2.154613466	31.70	43.81	24.49	3 mixed
Musophaga violacea	Musophagidae	1	56.31	78.63	44.39	2.184691884	31.40	43.85	24.75	4 fossil
Corythaeola cristata	Musophagidae	1	79.16	113.54	59.46	2.185447196	31.39	45.03	23.58	
Corythaixoides leucogaster	Musophagidae	1	49.32	72.83	42.55	2.339416058	29.95	44.22	25.83	
Corythaixoides concolor	Musophagidae	1	49.06	71.71	40.07	2.27843457	30.50	44.58	24.91	
Geococcyx californianus	Cuculidae	2	54.94	85.20	64.08	2.717145977	26.90	41.72	31.38	
Geococcyx velox	Cuculidae	2	49.72	72.77	53.54	2.540426388	28.25	41.34	30.42	
Guira guira	Cuculidae	3	37.27	57.61	40.76	2.639388248	27.48	42.47	30.05	
Tapera naevia	Cuculidae	3	27.47	41.59	31.73	2.669093557	27.25	41.26	31.48	
Dromococcyx phasianellus	Cuculidae	3	31.80	50.24	38.51	2.790880503	26.38	41.68	31.95	
Crotophaga major	Cuculidae	3	41.11	65.95	43.89	2.671855996	27.23	43.69	29.08	
Crotophaga ani	Cuculidae	3	35.90	57.49	38.94	2.686072423	27.13	43.44	29.43	
Crotophaga sulcirostris	Cuculidae	3	31.51	50.39	33.31	2.656299587	27.35	43.74	28.91	
Coccyzus longirostris	Cuculidae	1	38.83	55.39	37.36	2.388617049	29.51	42.10	28.39	
Coccycua minuta	Cuculidae	1	25.89	38.42	26.84	2.520664349	28.40	42.15	29.45	
Piaya cayana	Cuculidae	1	41.60	59.30	40.72	2.404326923	29.37	41.87	28.75	
Coccyzus americanus	Cuculidae	1	27.90	37.96	25.48	2.273835125	30.55	41.56	27.90	
Coccyzus melacoryphus	Cuculidae	1	28.26	40.10	26.09	2.342179759	29.92	42.46	27.62	
Coccyzus erythropthalmus	Cuculidae	3	26.76	37.85	24.31	2.322869955	30.09	42.57	27.34	
Coua cristata	Cuculidae	1	36.08	59.50	41.62	2.802660754	26.30	43.37	30.34	
Cacomantis flabelliformis	Cuculidae	1	22.17	30.63	20.15	2.290482634	30.39	41.99	27.62	
Cacomantis castaneiventris	Cuculidae	1	19.13	27.66	18.47	2.411395714	29.31	42.38	28.30	
Cuculus canorus	Cuculidae	3	28.69	39.12	22.55	2.149529453	31.75	43.29	24.96	
Cacomantis variolosus	Cuculidae	1	18.86	26.77	16.80	2.310180276	30.21	42.88	26.91	
Cacomantis sepulcralis	Cuculidae	1	17.57	25.23	15.92	2.34206033	29.92	42.97	27.11	
Chrysococcyx caprius	Cuculidae	1	19.11	27.16	17.41	2.332286761	30.01	42.65	27.34	
Chalcites minutillus	Cuculidae	1	18.05	26.78	17.75	2.467036011	28.84	42.79	28.36	
Chalcites lucidus	Cuculidae	1	18.70	27.08	17.98	2.409625668	29.33	42.47	28.20	
Chrysococcyx klaas	Cuculidae	1	17.62	25.15	15.62	2.3138479	30.18	43.07	26.75	
Centropus phasianinus	Cuculidae	3	57.21	78.85	55.31	2.345044573	29.89	41.20	28.90	
Centropus monachus	Cuculidae	3	49.80	70.55	49.22	2.40502008	29.37	41.61	29.03	
Centropus superciliosus	Cuculidae	3	42.62	59.55	40.17	2.339746598	29.94	41.84	28.22	
Ceuthmochares aereus	Cuculidae	3	31.60	43.72	28.54	2.286708861	30.43	42.10	27.48	
Rhamphococcyx calyorhynchu	Cuculidae	1	46.19	65.59	43.31	2.357653172	29.78	42.29	27.93	
Tetrax tetrax	Otididae	2	59.43	97.31	65.14	2.733467945	26.78	43.86	29.36	
Ardeotis arabs	Otididae	2	112.44	233.80	186.10	3.734436144	21.12	43.92	34.96	
Otis tarda	Otididae	2	126.46	216.80	153.20	2.925826348	25.47	43.67	30.86	
Chlamydotis undulata	Otididae	2	76.98	131.28	89.23	2.864510262	25.88	44.13	29.99	
Ardeotis kori	Otididae	2	121.06	246.20	194.90	3.643647778	21.53	43.80	34.67	
Foro panarium	Foratidae	4	54.10	88.40	61.30	2.767097967	26.55	43.38	30.08	

Table S2

Table S1

Raw palynomorph count data recorded from the John's Nose section. Related to Figure 3. Cretaceous-only taxa (K-taxa) are indicated by an asterisk. For notes on taxonomy and illustrations, see Nichols [S9] and Bercovici et al. [S10]. Stratigraphic position of each sample illustrated in Figure 3.

Table S2

Raw hindlimb measurements for extant and extinct Otidimorphae. Related to Figure 2.

Supplemental References

S1. Vajda, V., and McLoughlin, S. (2004). Fungal proliferation at the Cretaceous-Tertiary boundary. Science *303*, 1489.

S2. Ocampo, A., Vajda, V., and Buffetaut, E. (2006). Unravelling the Cretaceous-Paleogene (KT) catastrophe: Evidence from flora fauna and geology. Impact Series, 203-227.

S3. Ferrow, E., Vajda, V., Koch, C.B., Peucker-Ehrenbrink, B., and Willumsen, P.S. (2011). Multiproxy analysis of a new terrestrial and a marine Cretaceous–Paleogene (K–Pg) boundary site from New Zealand. Geochimica et Cosmochimica Acta *75*, 657-672.

S4. Vajda, V., Ocampo, A., Ferrow, E., and Koch, C.B. (2015). Nano particles as the primary cause for long-term sunlight suppression at high southern latitudes following the Chicxulub impact—evidence from ejecta deposits in Belize and Mexico. Gondwana Research *27*, 1079-1088.

S5. Vajda, V., Raine, J.I., and Hollis, C.J. (2001). Indication of global deforestation at the Cretaceous-Tertiary boundary by New Zealand fern spike. Science *294*, 1700-1702.

S6. Clyde, W.C., Ramezani, J., Johnson, K.R., Bowring, S.A., and Jones, M.M. (2016). Direct high-precision U–Pb geochronology of the end-Cretaceous extinction and calibration of Paleocene astronomical timescales. Earth and Planetary Science Letters *452*, 272-280.

S7. Prum, R.O., Berv, J.S., Dornburg, A., Field, D.J., Townsend, J.P., Lemmon, E.M., and Lemmon, A.R. (2015). A comprehensive phylogeny of birds (Aves) using targeted next-generation DNA sequencing. Nature *526*, 569-573.

S8. Claramunt, S., and Cracraft, J. (2015). A new time tree reveals Earth history's imprint on the evolution of modern birds. Science Advances *1*.

S9. Nichols, D.J. (2002). Palynology and palynostratigraphy of the Hell Creek Formation in North Dakota: a microfossil record of plants at the end of Cretaceous time. Geol. Soc. Am. Spec. Pap *361*, 393-456.

S10. Bercovici, A., Pearson, D., Nichols, D., and Wood, J. (2009). Biostratigraphy of selected K/T boundary sections in southwestern North Dakota, USA: toward a refinement of palynological identification criteria. Cretaceous Research *30*, 632-658.